was mainly based on reporter assays using a construct of the region from −188 to +83 of the h*NTCP* promoter, concluded that RAR did not affect h*NTCP* transcription (48). By using a reporter carrying a longer promoter region, our study is the first to implicate RARs in the regulation of h*NTCP* gene expression (Fig. 9). The turnover of NTCP protein was reported to be rapid, with a half-life of much less than 24 h (49). Consequently, reduction in the *NTCP* transcription by RAR inhibition could rapidly decrease the NTCP protein level and affect HBV susceptibility.

NTCP plays a major role in the hepatic influx of conjugated bile salts from portal circulation. Because NTCP knock-out mice are so far unavailable, it is not known whether loss of NTCP function can cause any physiological defect *in vivo*. However, no serious diseases are reported in individuals carrying single nucleotide polymorphisms that significantly decrease the transporter activity of NTCP (50, 51), suggesting that NTCP function may be redundant with other proteins. Organic anion transporting polypeptides are also known to be involved in bile acid transport. Moreover, an inhibition assay using Myrcludex-B showed that the IC_{50} value for HBV infection was ~0.1 nM (52), although that for NTCP transporter function was 4 nM (28), suggesting that HBV infection could be inhibited without fully inactivating the NTCP transporter (53). HBV entry inhibitors are expected to be useful for preventing *de novo* infection upon post-exposure prophylaxis or vertical transmission where serious toxicity might be avoided with a short term treatment (54). For drug development studies against HIV, down-regulation of the HIV coreceptor CCR5 by ribozymes could inhibit HIV infection both *in vitro* and *in vivo* (55). Disruption of CCR5 by zinc finger nucleases could reduce permissiveness to HIV infection and was effective in decreasing viral load *in vivo* (56). Thus, interventions to regulate viral permissiveness could become a method for eliminating viral infection (55). Our findings suggest that the regulatory mechanisms of NTCP expression could serve as targets for the development of anti-HBV agents. High throughput screening with a reporter assay using an *NTCP* promoter-driven reporter, as exemplified by this study, will be useful for identifying more anti-HBV drugs.

Acknowledgments—HepAD38 and HuS-E/2 cells were kindly provided by Dr. Christoph Seeger at Fox Chase Cancer Center and Dr. Kunitada Shimotohno at National Center for Global Health and Medicine. We are also grateful to all of the members of Department of Virology II, National Institute of Infectious Diseases.

REFERENCES

1. Liang, T. J. (2009) Hepatitis B: the virus and disease. *Hepatology* **49,** S13–S21
2. Ott, J. J., Stevens, G. A., Groeger, J., and Wiersma, S. T. (2012) Global epidemiology of hepatitis B virus infection: new estimates of age-specific HBsAg seroprevalence and endemicity. *Vaccine* **30,** 2212–2219
3. Zoulim, F., and Locarnini, S. (2013) Optimal management of chronic hepatitis B patients with treatment failure and antiviral drug resistance. *Liver Int.* **33,** Suppl. 1, 116–124
4. Arbuthnot, P., and Kew, M. (2001) Hepatitis B virus and hepatocellular carcinoma. *Int. J. Exp. Pathol.* **82,** 77–100
5. Kao, J. H., Chen, P. J., and Chen, D. S. (2010) Recent advances in the research of hepatitis B virus-related hepatocellular carcinoma: epidemiologic and molecular biological aspects. *Adv. Cancer Res.* **108,** 21–72
6. Lok, A. S. (2002) Chronic hepatitis B. *N. Engl. J. Med.* **346,** 1682–1683
7. Pagliaccetti, N. E., Chu, E. N., Bolen, C. R., Kleinstein, S. H., and Robek, M. D. (2010) λ and α interferons inhibit hepatitis B virus replication through a common molecular mechanism but with different *in vivo* activities. *Virology* **401,** 197–206
8. Robek, M. D., Boyd, B. S., and Chisari, F. V. (2005) λ interferon inhibits hepatitis B and C virus replication. *J. Virol.* **79,** 3851–3854
9. Dusheiko, G. (2013) Treatment of HBeAg positive chronic hepatitis B: interferon or nucleoside analogues. *Liver Int.* **33,** 137–150
10. Lau, G. K., Piratvisuth, T., Luo, K. X., Marcellin, P., Thongsawat, S., Cooksley, G., Gane, E., Fried, M. W., Chow, W. C., Paik, S. W., Chang, W. Y., Berg, T., Flisiak, R., McCloud, P., Pluck, N., and Peginterferon Alfa-2a HBeAg-Positive Chronic Hepatitis B Study Group. (2005) Peginterferon Alfa-2a, lamivudine, and the combination for HBeAg-positive chronic hepatitis B. *N. Engl. J. Med.* **352,** 2682–2695
11. Chen, L. P., Zhao, J., Du, Y., Han, Y. F., Su, T., Zhang, H. W., and Cao, G. W. (2012) Antiviral treatment to prevent chronic hepatitis B or C-related hepatocellular carcinoma. *World J. Virol.* **1,** 174–183
12. Ohishi, W., and Chayama, K. (2012) Treatment of chronic hepatitis B with nucleos(t)ide analogues. *Hepatol. Res.* **42,** 219–225
13. Liu, F., Wang, X., Wei, F., Hu, H., Zhang, D., Hu, P., and Ren, H. (2014) Efficacy and resistance in *de novo* combination lamivudine and adefovir dipivoxil therapy *versus* entecavir monotherapy for the treatment-naive patients with chronic hepatitis B: a meta-analysis. *Virol. J.* **11,** 59
14. Schulze, A., Gripon, P., and Urban, S. (2007) Hepatitis B virus infection initiates with a large surface protein-dependent binding to heparan sulfate proteoglycans. *Hepatology* **46,** 1759–1768
15. Yan, H., Zhong, G., Xu, G., He, W., Jing, Z., Gao, Z., Huang, Y., Qi, Y., Peng, B., Wang, H., Fu, L., Song, M., Chen, P., Gao, W., Ren, B., Sun, Y., Cai, T., Feng, X., Sui, J., and Li, W. (2012) Sodium taurocholate cotransporting polypeptide is a functional receptor for human hepatitis B and D virus. *Elife* **1,** e00049
16. Stieger, B. (2011) The role of the sodium-taurocholate cotransporting polypeptide (NTCP) and of the bile salt export pump (BSEP) in physiology and pathophysiology of bile formation. *Handb Exp. Pharmacol.* **201,** 205–259
17. Kotani, N., Maeda, K., Debori, Y., Camus, S., Li, R., Chesne, C., and Sugiyama, Y. (2012) Expression and transport function of drug uptake transporters in differentiated HepaRG cells. *Mol. Pharm.* **9,** 3434–3441
18. Kullak-Ublick, G. A., Beuers, U., and Paumgartner, G. (1996) Molecular and functional characterization of bile acid transport in human hepatoblastoma HepG2 cells. *Hepatology* **23,** 1053–1060
19. Watashi, K., Sluder, A., Daito, T., Matsunaga, S., Ryo, A., Nagamori, S., Iwamoto, M., Nakajima, S., Tsukuda, S., Borroto-Esoda, K., Sugiyama, M., Tanaka, Y., Kanai, Y., Kusuhara, H., Mizokami, M., and Wakita, T. (2014) Cyclosporin A and its analogs inhibit hepatitis B virus entry into cultured hepatocytes through targeting a membrane transporter, sodium taurocholate cotransporting polypeptide (NTCP). *Hepatology* **59,** 1726–1737
20. Gripon, P., Cannie, I., and Urban, S. (2005) Efficient inhibition of hepatitis B virus infection by acylated peptides derived from the large viral surface protein. *J. Virol.* **79,** 1613–1622
21. Petersen, J., Dandri, M., Mier, W., Lütgehetmann, M., Volz, T., von Weizsäcker, F., Haberkorn, U., Fischer, L., Pollok, J. M., Erbes, B., Seitz, S., and Urban, S. (2008) Prevention of hepatitis B virus infection *in vivo* by entry inhibitors derived from the large envelope protein. *Nat. Biotechnol.* **26,** 335–341
22. Ladner, S. K., Otto, M. J., Barker, C. S., Zaifert, K., Wang, G. H., Guo, J. T., Seeger, C., and King, R. W. (1997) Inducible expression of human hepatitis B virus (HBV) in stably transfected hepatoblastoma cells: a novel system for screening potential inhibitors of HBV replication. *Antimicrob. Agents Chemother.* **41,** 1715–1720
23. Aly, H. H., Watashi, K., Hijikata, M., Kaneko, H., Takada, Y., Egawa, H., Uemoto, S., and Shimotohno, K. (2007) Serum-derived hepatitis C virus infectivity in interferon regulatory factor-7-suppressed human primary hepatocytes. *J. Hepatol.* **46,** 26–36
24. Sugiyama, M., Tanaka, Y., Kato, T., Orito, E., Ito, K., Acharya, S. K., Gish,

R. G., Kramvis, A., Shimada, T., Izumi, N., Kaito, M., Miyakawa, Y., and Mizokami, M. (2006) Influence of hepatitis B virus genotypes on the intra- and extracellular expression of viral DNA and antigens. *Hepatology* **44,** 915–924

25. Watashi, K., Hijikata, M., Tagawa, A., Doi, T., Marusawa, H., and Shimotohno, K. (2003) Modulation of retinoid signaling by a cytoplasmic viral protein via sequestration of Sp110b, a potent transcriptional corepressor of retinoic acid receptor, from the nucleus. *Mol. Cell. Biol.* **23,** 7498–7509
26. Marusawa, H., Hijikata, M., Watashi, K., Chiba, T., and Shimotohno, K. (2001) Regulation of Fas-mediated apoptosis by NF-κB activity in human hepatocyte derived cell lines. *Microbiol. Immunol.* **45,** 483–489
27. Watashi, K., Khan, M., Yedavalli, V. R., Yeung, M. L., Strebel, K., and Jeang, K. T. (2008) Human immunodeficiency virus type 1 replication and regulation of APOBEC3G by peptidyl prolyl isomerase Pin1. *J. Virol.* **82,** 9928–9936
28. Ni, Y., Lempp, F. A., Mehrle, S., Nkongolo, S., Kaufman, C., Fälth, M., Stindt, J., Königer, C., Nassal, M., Kubitz, R., Sültmann, H., and Urban, S. (2014) Hepatitis B and D viruses exploit sodium taurocholate co-transporting polypeptide for species-specific entry into hepatocytes. *Gastroenterology* **146,** 1070–1083
29. Gripon, P., Rumin, S., Urban, S., Le Seyec, J., Glaise, D., Cannie, I., Guyomard, C., Lucas, J., Trepo, C., and Guguen-Guillouzo, C. (2002) Infection of a human hepatoma cell line by hepatitis B virus. *Proc. Natl. Acad. Sci. U.S.A.* **99,** 15655–15660
30. Cattaneo, R., Will, H., and Schaller, H. (1984) Hepatitis B virus transcription in the infected liver. *EMBO J.* **3,** 2191–2196
31. Hirsch, R. C., Lavine, J. E., Chang, L. J., Varmus, H. E., and Ganem, D. (1990) Polymerase gene products of hepatitis B viruses are required for genomic RNA packaging as well as for reverse transcription. *Nature* **344,** 552–555
32. Huan, B., and Siddiqui, A. (1993) Regulation of hepatitis B virus gene expression. *J. Hepatol.* **17,** S20–S23
33. Newman, M., Suk, F. M., Cajimat, M., Chua, P. K., and Shih, C. (2003) Stability and morphology comparisons of self-assembled virus-like particles from wild-type and mutant human hepatitis B virus capsid proteins. *J. Virol.* **77,** 12950–12960
34. Yeh, C. T., and Ou, J. H. (1991) Phosphorylation of hepatitis B virus precore and core proteins. *J. Virol.* **65,** 2327–2331
35. Nkongolo, S., Ni, Y., Lempp, F. A., Kaufman, C., Lindner, T., Esser-Nobis, K., Lohmann, V., Mier, W., Mehrle, S., and Urban, S. (2014) Cyclosporin A inhibits hepatitis B and hepatitis D virus entry by cyclophilin-independent interference with the NTCP receptor. *J. Hepatol.* **65,** 723–731
36. Sells, M. A., Zelent, A. Z., Shvartsman, M., and Acs, G. (1988) Replicative intermediates of hepatitis B virus in HepG2 cells that produce infectious virions. *J. Virol.* **62,** 2836–2844
37. Watashi, K., Liang, G., Iwamoto, M., Marusawa, H., Uchida, N., Daito, T., Kitamura, K., Muramatsu, M., Ohashi, H., Kiyohara, T., Suzuki, R., Li, J., Tong, S., Tanaka, Y., Murata, K., Aizaki, H., and Wakita, T. (2013) Interleukin-1 and tumor necrosis factor-α trigger restriction of hepatitis B virus infection via a cytidine deaminase activation-induced cytidine deaminase (AID). *J. Biol. Chem.* **288,** 31715–31727
38. Apfel, C., Bauer, F., Crettaz, M., Forni, L., Kamber, M., Kaufmann, F., LeMotte, P., Pirson, W., and Klaus, M. (1992) A retinoic acid receptor α antagonist selectively counteracts retinoic acid effects. *Proc. Natl. Acad. Sci. U.S.A.* **89,** 7129–7133
39. Denson, L. A., Sturm, E., Echevarria, W., Zimmerman, T. L., Makishima, M., Mangelsdorf, D. J., and Karpen, S. J. (2001) The orphan nuclear receptor, shp, mediates bile acid-induced inhibition of the rat bile acid transporter, ntcp. *Gastroenterology* **121,** 140–147
40. Bastien, J., and Rochette-Egly, C. (2004) Nuclear retinoid receptors and the transcription of retinoid-target genes. *Gene* **328,** 1–16
41. Ishida, Y., Yamasaki, C., Yanagi, A., Yoshizane, Y., Chayama, K., and Tateno, C. (2013) *International Meeting on Molecular Biology of Hepatitis B Virus* **P13**
42. Yan, H., Peng, B., Liu, Y., Xu, G., He, W., Ren, B., Jing, Z., Sui, J., and Li, W. (2014) Viral entry of hepatitis B and D viruses and bile salts transportation share common molecular determinants on sodium taurocholate cotransporting polypeptide. *J. Virol.* **88,** 3273–3284
43. Iwamoto, M., Watashi, K., Tsukuda, S., Aly, H. H., Fukasawa, M., Fujimoto, A., Suzuki, R., Aizaki, H., Ito, T., Koiwai, O., Kusuhara, H., and Wakita, T. (2014) Evaluation and identification of hepatitis B virus entry inhibitors using HepG2 cells overexpressing a membrane transporter NTCP. *Biochem. Biophys. Res. Commun.* **443,** 808–813
44. Shiao, T., Iwahashi, M., Fortune, J., Quattrochi, L., Bowman, S., Wick, M., Qadri, I., and Simon, F. R. (2000) Structural and functional characterization of liver cell-specific activity of the human sodium/taurocholate cotransporter. *Genomics* **69,** 203–213
45. Huan, B., and Siddiqui, A. (1992) Retinoid X receptor RXRα binds to and trans-activates the hepatitis B virus enhancer. *Proc. Natl. Acad. Sci. U.S.A.* **89,** 9059–9063
46. Geier, A., Martin, I. V., Dietrich, C. G., Balasubramaniyan, N., Strauch, S., Suchy, F. J., Gartung, C., Trautwein, C., and Ananthanarayanan, M. (2008) Hepatocyte nuclear factor-4α is a central transactivator of the mouse Ntcp gene. *Am. J. Physiol. Gastrointest. Liver Physiol.* **295,** G226–G233
47. Zollner, G., Wagner, M., Fickert, P., Geier, A., Fuchsbichler, A., Silbert, D., Gumhold, J., Zatloukal, K., Kaser, A., Tilg, H., Denk, H., and Trauner, M. (2005) Role of nuclear receptors and hepatocyte-enriched transcription factors for Ntcp repression in biliary obstruction in mouse liver. *Am. J. Physiol. Gastrointest. Liver Physiol.* **289,** G798–G805
48. Jung, D., Hagenbuch, B., Fried, M., Meier, P. J., and Kullak-Ublick, G. A. (2004) Role of liver-enriched transcription factors and nuclear receptors in regulating the human, mouse, and rat NTCP gene. *Am. J. Physiol. Gastrointest. Liver Physiol.* **286,** G752–G761
49. Rippin, S. J., Hagenbuch, B., Meier, P. J., and Stieger, B. (2001) Cholestatic expression pattern of sinusoidal and canalicular organic anion transport systems in primary cultured rat hepatocytes. *Hepatology* **33,** 776–782
50. Ho, R. H., Leake, B. F., Roberts, R. L., Lee, W., and Kim, R. B. (2004) Ethnicity-dependent polymorphism in Na^+-taurocholate cotransporting polypeptide (SLC10A1) reveals a domain critical for bile acid substrate recognition. *J. Biol. Chem.* **279,** 7213–7222
51. Pan, W., Song, I. S., Shin, H. J., Kim, M. H., Choi, Y. L., Lim, S. J., Kim, W. Y., Lee, S. S., and Shin, J. G. (2011) Genetic polymorphisms in Na^+-taurocholate co-transporting polypeptide (NTCP) and ileal apical sodium-dependent bile acid transporter (ASBT) and ethnic comparisons of functional variants of NTCP among Asian populations. *Xenobiotica* **41,** 501–510
52. Schulze, A., Schieck, A., Ni, Y., Mier, W., and Urban, S. (2010) Fine mapping of pre-S sequence requirements for hepatitis B virus large envelope protein-mediated receptor interaction. *J. Virol.* **84,** 1989–2000
53. Watashi, K., Urban, S., Li, W., and Wakita, T. (2014) NTCP and beyond: opening the door to unveil hepatitis B virus entry. *Int. J. Mol. Sci.* **15,** 2892–2905
54. Deuffic-Burban, S., Delarocque-Astagneau, E., Abiteboul, D., Bouvet, E., and Yazdanpanah, Y. (2011) Blood-borne viruses in health care workers: prevention and management. *J. Clin. Virol.* **52,** 4–10
55. Bai, J., Gorantla, S., Banda, N., Cagnon, L., Rossi, J., and Akkina, R. (2000) Characterization of anti-CCR5 ribozyme-transduced $CD34^+$ hematopoietic progenitor cells *in vitro* and in a SCID-hu mouse model *in vivo*. *Mol. Ther.* **1,** 244–254
56. Perez, E. E., Wang, J., Miller, J. C., Jouvenot, Y., Kim, K. A., Liu, O., Wang, N., Lee, G., Bartsevich, V. V., Lee, Y. L., Guschin, D. Y., Rupniewski, I., Waite, A. J., Carpenito, C., Carroll, R. G., Orange, J. S., Urnov, F. D., Rebar, E. J., Ando, D., Gregory, P. D., Riley, J. L., Holmes, M. C., and June, C. H. (2008) Establishment of HIV-1 resistance in $CD4^+$ T cells by genome editing using zinc-finger nucleases. *Nat. Biotechnol.* **26,** 808–816

JOBNAME: AUTHOR QUERIES PAGE: 1 SESS: 1 OUTPUT: Mon Jan 19 09:46:20 2015
/tapraid4/zbc-bc/zbc-bc/zbc01115/zbc0943-15z

AUTHOR QUERIES

AUTHOR PLEASE ANSWER ALL QUERIES 1

A—Au: do you mean Ro41-5253 instead of -5263?

Yes that's right. I corrected it in my proof.

JVI
Journals.ASM.org

Targeting Cellular Squalene Synthase, an Enzyme Essential for Cholesterol Biosynthesis, Is a Potential Antiviral Strategy against Hepatitis C Virus

Kyoko Saito,[a] Yoshitaka Shirasago,[a,b] Tetsuro Suzuki,[c] Hideki Aizaki,[d] Kentaro Hanada,[a] Takaji Wakita,[d] Masahiro Nishijima,[e] Masayoshi Fukasawa[a]

Department of Biochemistry and Cell Biology, National Institute of Infectious Diseases, Tokyo, Japan[a]; Graduate School of Biological Science, Tokyo University of Science, Chiba, Japan[b]; Department of Infectious Diseases, Hamamatsu University School of Medicine, Shizuoka, Japan[c]; Department of Virology II, National Institute of Infectious Diseases, Tokyo, Japan[d]; Showa Pharmaceutical University, Tokyo, Japan[e]

ABSTRACT

Hepatitis C virus (HCV) exploits host membrane cholesterol and its metabolism for progeny virus production. Here, we examined the impact of targeting cellular squalene synthase (SQS), the first committed enzyme for cholesterol biosynthesis, on HCV production. By using the HCV JFH-1 strain and human hepatoma Huh-7.5.1-derived cells, we found that the SQS inhibitors YM-53601 and zaragozic acid A decreased viral RNA, protein, and progeny production in HCV-infected cells without affecting cell viability. Similarly, small interfering RNA (siRNA)-mediated knockdown of SQS led to significantly reduced HCV production, confirming the enzyme as an antiviral target. A metabolic labeling study demonstrated that YM-53601 suppressed the biosynthesis of cholesterol and cholesteryl esters at antiviral concentrations. Unlike YM-53601, the cholesterol esterification inhibitor Sandoz 58-035 did not exhibit an antiviral effect, suggesting that biosynthesis of cholesterol is more important than that of cholesteryl esters for HCV production. YM-53601 inhibited transient replication of a JFH-1 subgenomic replicon and entry of JFH-1 pseudoparticles, suggesting that at least suppression of viral RNA replication and entry contributes to the antiviral effect of the drug. Collectively, our findings highlight the importance of the cholesterol biosynthetic pathway in HCV production and implicate SQS as a potential target for antiviral strategies against HCV.

IMPORTANCE

Hepatitis C virus (HCV) is known to be closely associated with host cholesterol and its metabolism throughout the viral life cycle. However, the impact of targeting cholesterol biosynthetic enzymes on HCV production is not fully understood. We found that squalene synthase, the first committed enzyme for cholesterol biosynthesis, is important for HCV production, and we propose this enzyme as a potential anti-HCV target. We provide evidence that synthesis of free cholesterol is more important than that of esterified cholesterol for HCV production, highlighting a marked free cholesterol dependency of HCV production. Our findings also offer a new insight into a role of the intracellular cholesterol pool that is coupled to its biosynthesis in the HCV life cycle.

Hepatitis C virus (HCV) is a causative agent of acute and chronic hepatitis, which can eventually lead to cirrhosis and hepatocellular carcinoma. HCV infection is recognized as a major threat to global public health, with 130 to 150 million people worldwide being infected with the virus (1). Over the last decade, the standard therapy for chronic HCV infection has been a combination of pegylated interferon alpha and ribavirin (2), but that has greatly changed after the emergence of first direct-acting antivirals that selectively target HCV, i.e., telaprevir and boceprevir (3, 4). These drugs, both used in combination with pegylated interferon and ribavirin, have brought significant benefits to patients who did not respond to the conventional therapy. In addition, recent clinical data on the newly approved direct-acting antivirals simeprevir and sofosbuvir have provided novel insights on combination therapies with inhibitors of multiple targets (5). However, direct-acting antivirals are frequently associated with the emergence of drug-resistant HCV variants, likely leading to treatment failure (6). Thus, development of host-targeted agents, which are expected to have a high genetic barrier to resistance, should be encouraged to expand treatment options for chronic hepatitis C.

HCV is an enveloped, positive-sense, single-stranded RNA virus belonging to the *Hepacivirus* genus of the *Flaviviridae* family. The HCV genome is 9.6 kb in length and contains a single open reading frame encoding a large polyprotein of approximately 3,000 amino acids. Translation of the polyprotein is directed by an internal ribosome entry site (IRES) located mostly in the highly conserved 5′ untranslated region (7). The polyprotein is co- and posttranslationally processed into three structural proteins (core, E1, and E2), a small ion channel protein (p7), and six nonstructural proteins (NS2, NS3, NS4A, NS4B, NS5A, and NS5B) by cel-

Received 24 November 2014 **Accepted** 26 November 2014
Accepted manuscript posted online 3 December 2014
Citation Saito K, Shirasago Y, Suzuki T, Aizaki H, Hanada K, Wakita T, Nishijima M, Fukasawa M. 2015. Targeting cellular squalene synthase, an enzyme essential for cholesterol biosynthesis, is a potential antiviral strategy against hepatitis C virus. J Virol 89:2220–2232. doi:10.1128/JVI.03385-14.
Editor: S. Perlman
Address correspondence to Masayoshi Fukasawa, fuka@nih.go.jp.

doi:10.1128/JVI.03385-14

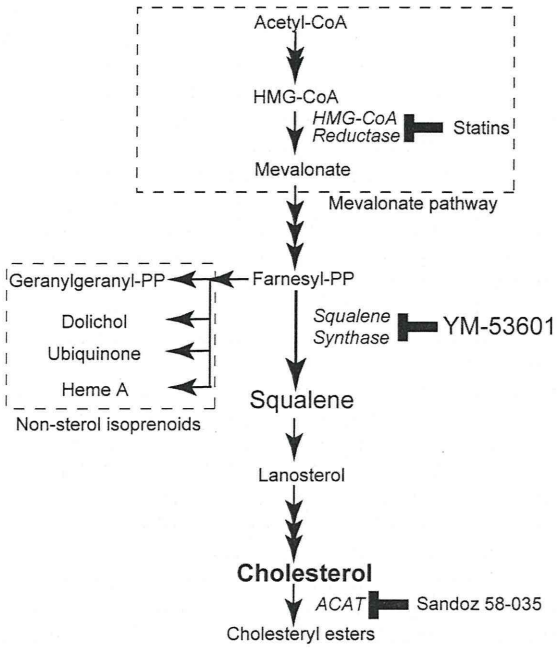

FIG 1 Cholesterol biosynthetic pathway in mammalian cells. Enzymes are shown in italics; inhibitors for the enzymes are shown next to the enzymes. Abbreviations: CoA, coenzyme A; HMG, 3-hydroxy-3-methylglutaryl; PP, pyrophosphate; ACAT, acyl-CoA:cholesterol acyltransferase.

lular and viral proteases (8–10). The nonstructural proteins assemble on the endoplasmic reticulum (ER)-derived membranes and recruit the viral genome into an RNA replication complex (11, 12).

Several lines of evidence suggest that HCV is closely associated with cholesterol and its metabolism throughout the viral life cycle in hepatocytes (13). In a previous study using a cholesterol-extracting drug, methyl-β-cyclodextrin, HCV entry was found to be in part dependent on the host membrane cholesterol content (14). Biochemical studies suggest that HCV RNA replication takes place on lipid rafts (15–17), i.e., detergent-resistant membrane microdomains enriched in cholesterol and sphingolipids (18). Lipid rafts also appear to be involved in HCV virion assembly because the viral structural proteins are associated with them (19, 20). Virion assembly occurs at the ER membranes immediately adjacent to the lipid droplet (21, 22), a major storage organelle for cholesteryl esters and triglycerides. Subsequent maturation and release of viral particles are tightly linked to the very-low-density lipoprotein (VLDL) secretion pathway (reference 22 and references therein; 23). Indeed, the lipid composition of secreted viral particles resembles that of VLDLs and low-density lipoproteins (LDLs), with a large amount of cholesteryl esters (24). The viral particles are also enriched in cholesterol and sphingomyelin, both of which are important for particle maturation and infectivity (19).

Cholesterol is synthesized from acetyl coenzyme A (acetyl-CoA) via a series of enzymatic reactions shown in Fig. 1. The rate-limiting enzyme of the cholesterol biosynthetic pathway is 3-hydroxy-3-methylglutaryl (HMG)-CoA reductase, which catalyzes the synthesis of mevalonate (25). Previous studies have shown that HMG-CoA reductase inhibitors or statins (26) block viral RNA replication in HCV genotype 1b replicon cells (27–29). Although statins are widely used as cholesterol-lowering drugs (30), their anti-HCV effect has been attributed not to a decrease in cholesterol content but rather to decreases of the nonsterol isoprenoids geranylgeranyl lipids (27, 28), the biosynthetic pathway of which shares early steps with that of cholesterol (Fig. 1). Although recent studies have shown that downstream enzymes in the cholesterol biosynthetic pathway, such as oxidosqualene cyclase, lanosterol C_{14}-demethylase, 24-dehydrocholesterol reductase, and 7-dehydrocholesterol reductase, are required for HCV production (31–33), the role of the committed steps of cholesterol biosynthesis in the HCV life cycle is not fully understood.

In this study, we focused on squalene synthase (SQS), which is the first committed enzyme in cholesterol biosynthesis (34) (Fig. 1). We examined the impact of SQS inhibition on HCV production by using an HCV cell culture system with human hepatoma Huh-7.5.1-derived cells and an HCV genotype 2a isolate, JFH-1 (35–37). We present data showing that SQS-mediated cholesterol biosynthesis is important for viral production, and we propose that SQS is a potential anti-HCV target.

MATERIALS AND METHODS

Reagents. YM-53601 (38), zaragozic acid A (39), and Sandoz 58-035 (40) were purchased from Sigma-Aldrich Corp. (St. Louis, MO, USA) and dissolved in dimethyl sulfoxide (DMSO). A Stealth RNA interference (RNAi) small interfering RNA (siRNA) for human SQS, HSS103617 (siSQS), and a Stealth RNAi negative-control low-GC duplex (siCONT) were purchased from Life Technologies Corp. (Carlsbad, CA, USA). Human low-density lipoprotein was purchased from Biomedical Technologies, Inc. (Stoughton, MA, USA). [*methyl*-^{3}H]acetate was purchased from Moravek Biochemicals, Inc. (Brea, CA, USA).

Cell culture. A highly HCV-permissive subclonal cell line derived from Huh-7.5.1 cells (36), Huh-7.5.1-8 (37), was maintained at 37°C and 5% CO_2 in Dulbecco's modified Eagle's medium that contained 10% fetal bovine serum, 0.1 mM nonessential amino acids, 100 units/ml penicillin G, and 100 μg/ml streptomycin sulfate (referred to as "complete medium"). Serum-free culture was performed as described previously (41) with slight modifications: Huh-7.5.1-8 cells were incubated at 37°C and 5% CO_2 in Dulbecco's modified Eagle's medium that contained 1% Nutridoma-SP (Roche Applied Science, Penzberg, Upper Bavaria, Germany) and 25 μg/ml gentamicin (referred to as "serum-free medium").

Virus stock and infection. HCV JFH-1 was prepared from culture supernatants of Huh-7.5.1-8 cells that had been transfected with *in vitro*-transcribed JFH-1 RNA as previously described (35). After serial passages of the JFH-1 virus in naive Huh-7.5.1-8 cells, infectious culture supernatants were collected and used as viral stocks in this study. Virus titers were determined by fluorescent-focus assays as previously described (42). For infection, cells were incubated with the virus at a multiplicity of infection of 4 fluorescent-focus-forming units/cell in complete medium for 2 h at 37°C.

Immunoblotting. Cells were lysed in NuPAGE lithium dodecyl sulfate (LDS) sample buffer (Life Technologies Corp.) that contained 0.05 M dithiothreitol (DTT) and then heated at 95°C for 5 min. The resultant lysates were subjected to SDS-polyacrylamide gel electrophoresis on NuPAGE 4 to 12% Bis-Tris gels (Life Technologies Corp.) and then transferred to Immun-Blot polyvinylidene difluoride membranes (Bio-Rad Laboratories, Inc., Hercules, CA, USA) according to the manufacturer's protocols. After being blocked with 5% (wt/vol) skim milk in TBS-T (0.05 M Tris-HCl [pH 7.6], 0.15 M NaCl, 0.1% [vol/vol] Tween 20), the membranes were probed with 1:5,000 dilutions of anti-HCV core monoclonal antibody (B2; Anogen, Yes Biotech Laboratories, Ltd., Mississauga, Ontario, Canada) or anti-HCV NS3 monoclonal antibody (8G-2; Abcam, Plc., Cambridge, United Kingdom) or with a 1:10,000 dilution of anti-glyceraldehyde-3-phosphate dehydrogenase (anti-GAPDH) monoclonal antibody (6C5; Abcam, Plc.), followed by a 1:5,000 dilution of horseradish

peroxidase-conjugated AffiniPure goat anti-mouse IgG(H+L) (Jackson ImmunoResearch Laboratories, Inc., West Grove, PA, USA) in TBS-T that contained 2% (wt/vol) skim milk. For detection of SQS, the membranes were probed with a 1:5,000 dilution of anti-SQS polyclonal antibody (B01; Abnova Corp., Taipei City, Taiwan) followed by a 1:5,000 dilution of horseradish peroxidase-conjugated AffiniPure goat anti-rabbit IgG(H+L) (Jackson ImmunoResearch Laboratories, Inc.). Each protein band complexed with the antibody on the membrane was visualized with an enhanced chemiluminescence immunoblotting detection system (GE Healthcare, UK Ltd., Little Chalfont, United Kingdom; Merck Millipore, Billerica, USA) and quantified using Image J 1.440 software (National Institutes of Health, Bethesda, MD, USA).

RT-qPCR analysis. Total RNA was isolated from cells by using an RNeasy Plus minikit (Qiagen, GmbH, Hilden, Germany) and reverse transcribed by random hexamer primers using a Transcriptor first-strand cDNA synthesis kit (Roche Applied Science) according to the manufacturer's protocols. Quantitative reverse transcription-PCR (RT-qPCR) was carried out on the LightCycler system (Roche Applied Science) using LightCycler FastStart DNA Master SYBR green I (Roche Applied Science) and specific primers for the core sequence (5′-CGCAACGTGGGTAAAG TCATCG-3′ and 5′-CGGGTAGGTTCCCTGTTGCATAA-3′), the NS5B sequence (5′-CAAGGGTCAAACCTGCGGTTACA-3′ and 5′-TGACTA CTAGGTCATCGCCGCATAC-3′), or the human GAPDH sequence (Search–LC, GmbH, Heidelberg, Germany). The relative amounts of viral RNA were calculated by dividing the copy number of a viral transcript by that of a GAPDH transcript in the same sample.

Metabolic labeling of lipids with radioactive acetate and TLC. Cells were plated at 1×10^5 cells per well of a 6-well plate 1 day before labeling and then incubated with [^{3}H]acetate (1.85 MBq/well) in serum-free medium for various periods. The cells were washed and harvested with phosphate-buffered saline (PBS), and a lipid fraction was extracted from the cells according to the method of Bligh and Dyer (43). The lipid fraction was spotted on a silica gel 60 plate (Merck Millipore) and separated by thin-layer chromatography (TLC) using hexane-diethyl ether-acetate (70:30:1, vol/vol/vol). The incorporation of ^{3}H radioactivity into each lipid was quantified using a BAS-1800 Bio-Image Analyzer (Fujifilm Corp.) or a Typhoon FLA 7000 biomolecular imager (GE Healthcare, UK Ltd.) and then normalized with the protein levels.

Determination of cholesterol and cholesteryl ester contents. Cells were disrupted in PBS by sonication. The lipid fraction was extracted from the cells as described above. The content of cholesterol in the lipid fraction was determined by an enzymatic colorimetric method using the Wako free cholesterol E test (Wako Pure Chemical Industries, Ltd., Osaka, Japan) according to the manufacturer's protocol and then normalized with the protein levels. The content of cholesteryl esters in the lipid fraction was determined by a direct measurement method for the enzymatic determination of cholesteryl esters as described elsewhere (44) and then normalized with the protein levels.

siRNA transfection. Cells were plated at 3×10^4 cells per well in 24-well plates 2 days before transfection and grown in complete medium. siRNA was complexed with Lipofectamine RNAiMAX transfection reagent (Life Technologies Corp.) according to the manufacturer's protocol and then added to the cells at a final concentration of 5 nM. After 5 h of incubation, the cells were washed and then placed in serum-free medium.

Subgenomic replicon plasmids. The HCV subgenomic replicon plasmids used in this study contain the T7 promoter followed by a bicistronic replicon sequence; the first is a part of the core region fused to either the luciferase (*luc*) gene of the firefly *Photinus pyralis* or the neomycin phosphotransferase (*neo*) gene translated under the control of the HCV IRES, and the second is the NS3-NS5B-coding region translated under the control of the encephalomyocarditis virus (EMCV) IRES. Subgenomic replicon plasmids of the JFH-1 strain, pSGR-JFH1/Luc and pSGR-JFH1/Luc-GND (45), carry the *luc* gene; the latter contains a GDD-to-GND mutation in NS5B, which abolishes RNA polymerase activity. Subgenomic replicon plasmids of the Con-1 strain (genotype 1b), pFK-I_{389}Luci/NS3-3′/NK5.1 and pFK-I_{389}neo/NS3-3′/NK5.1/ΔGDD (46), were kindly provided by Ralf Bartenschlager (University of Heidelberg, Germany) and carry the *luc* gene and the *neo* gene, respectively; the latter contains a deletion in the GDD active site of NS5B that abolishes RNA polymerase activity. A replication-incompetent mutant of pFK-I_{389}Luci/NS3-3′/NK5.1 was prepared by replacing an AscI-PmeI fragment that codes for the *neo* gene of pFK-I_{389}neo/NS3-3′/NK5.1/ΔGDD with the corresponding fragment that codes for the *luc* gene from pFK-I_{389}Luci/NS3-3′/NK5.1 (referred to as pFK-I_{389}/Luci/NS3-3′/NK5.1/ΔGDD).

***In vitro* transcription of RNA.** Linearization of plasmids, *in vitro* transcription with T7 RNA polymerase, and RNA purification were performed as previously described (47) except that the AmpliScribe T7 high-yield transcription kit (Epicentre Biotechnologies Corp., Madison, WI, USA) was used.

Transfection with *in vitro*-transcribed RNA. Electroporation was performed as described previously (48) with slight modifications. Cells (1×10^7 to 2×10^7) were mixed with 20 to 25 μg of *in vitro*-transcribed RNA in K-PBS (30 mM NaCl, 120 mM KCl, 8 mM Na_2HPO_4, 1.5 mM KH_2PO_4, and 5 mM $MgCl_2$, pH 7.9) and then pulsed at 975 μF and 290 V in a cuvette with a gap width of 0.4 cm by using a Gene Pulser Xcell system (Bio-Rad Laboratories, Inc.). For lipofection, cells were plated at 3×10^4 cells per well in a 24-well plate 2 days before transfection. The cells were then transfected with 0.5 μg of *in vitro*-transcribed RNA for 3 h using the TransMessenger transfection reagent (Qiagen, GmbH) according to the manufacturer's protocol.

Luciferase assay. Cells were lysed with cell culture lysis reagent (Promega Corp., Madison, WI, USA). Five microliters of the lysate was mixed with 25 μl of luciferase assay reagent (Promega Corp.), and then luciferase activity in the lysate was measured by using a Luminescencer-PSN luminometer (Atto Corp., Tokyo, Japan).

Preparation of HA-tagged NS4B-expressing cells. An expression plasmid that encodes NS4B protein N-terminally fused to a hemagglutinin (HA) tag sequence followed by a tobacco etch virus (TEV) protease cleavage site, pCXN2/HA-TEV-NS4B, was previously described (49). Huh-7.5.1-8 cells were transfected with pCXN2/HA-TEV-NS4B using FuGENE 6 transfection reagent (Roche Applied Science) and grown in the presence of 500 μg/ml of G418. G418-resistant cells were cloned by limiting dilution, and expression of HA-tagged NS4B protein in each clone was confirmed by immunoblotting with a rat anti-HA monoclonal antibody (clone 3F10; Roche Applied Science). Similarly, Huh-7.5.1-8 cells were transfected with a backbone plasmid, a modified version of pCXN2 (50, 51). The resultant G418-resistant cells were cloned and used as a negative control.

Immunofluorescence analysis. Cells grown on collagen-coated coverslips (Asahi Glass Co., Ltd., Japan) were fixed with 4% paraformaldehyde phosphate buffer solution (Wako Pure Chemical Industries, Ltd.) for 15 min at room temperature. After being washed with 30 mM glycine in PBS, the cells were permeabilized with 0.2% Triton X-100 in PBS for 10 min at room temperature and then blocked with 3% (wt/vol) bovine serum albumin (BSA) in PBS. The cells were incubated with the anti-HA rat monoclonal antibody diluted 1:500 with 1% (wt/vol) BSA in PBS followed by an Alexa Fluor 488 goat anti-rat IgG(H+L) antibody (Life Technologies Corp.) diluted 1:300 with the same solution. The cells were mounted with ProLong Diamond antifade mountant with 4′,6-diamidino-2-phenylindole (DAPI) (Life Technologies Corp.) and observed using a confocal microscope (LSM 700; Carl Zeiss Microscopy, GmbH, Jena, Germany) equipped with an oil immersion objective lens (Plan-Apochromat 40×/1.4 oil DIC M27; Carl Zeiss Microscopy, GmbH).

Preparation of and infection with HCVpp. HCV pseudoparticles (HCVpp) were prepared as described previously (52, 53) with slight modifications. Briefly, HEK293T cells were transfected with a Gag-Pol packaging plasmid (Gag-Pol 5349), a reporter (luciferase) plasmid (Luc 126), and a pcDNA3.1(+) (Life Technologies Corp.)-based expression plasmid that encodes HCV envelope proteins (E1 and E2) of the JFH-1 strain (genotype 2a) or the TH strain (54) (genotype 1b) for 24 h using the

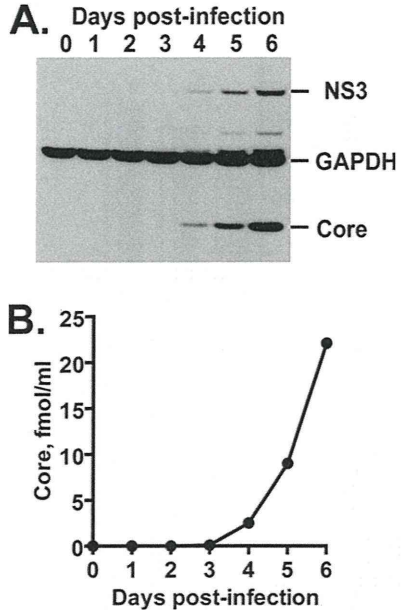

FIG 2 HCV production in Huh-7.5.1-8 cells grown under serum-free conditions. Huh-7.5.1-8 cells were infected with HCV JFH-1 and then cultured in serum-free medium. (A) The cells were harvested at the indicated time points. Each cell lysate (15 μg of protein) was subjected to immunoblotting for core, NS3, and GAPDH proteins. (B) Culture supernatants were harvested at the indicated time points. The amount of secreted viral particles in each supernatant was determined by measuring the amount of core protein by ELISA. The results from one of two independent experiments with similar results are shown.

X-treme Gene HP DNA transfection reagent (Roche Applied Science), and then the medium was replaced with serum-free medium that contained 0.1 mM nonessential amino acids. HCVpp-containing medium was collected after additional 24 to 36 h of culture and used as HCVpp stock. In parallel, HEK293T cells were similarly transfected, except that the envelope protein-expressing plasmid was replaced with pcDNA3.1(+), and their culture medium was used as a negative control. For infection, Huh-7.5.1-8 cells were plated at 6×10^4 cells per well of a 48-well plate and grown in serum-free medium for 2 days. The cells were then infected with HCVpp for 6 h at 37°C. After being washed, the cells were grown in complete medium for an additional 3 days and assayed for luciferase activity.

Other methods. Protein concentrations were measured using the bicinchoninic acid (BCA) protein assay reagent (Thermo Fisher Scientific, Inc., Waltham, MA, USA) with BSA as a standard. The amount of viral core protein in a culture supernatant, which is the hallmark of the secreted virus level, was quantified using the Ortho HCV antigen enzyme-linked immunosorbent assay (ELISA) (Ortho-Clinical Diagnostics, Inc., Raritan, NJ, USA). Cell viability was determined by using the XTT cell proliferation kit II (Roche Applied Science). The 50% inhibitory concentration (IC_{50}) was calculated by using the equation "log (inhibitor) versus normalized response" of the nonlinear regression model included in GraphPad Prism 5 (GraphPad Software, Inc., La Jolla, CA, USA). Statistical analysis was performed by Student's *t* test using the GraphPad calculator (QuickCalcs); differences with a *P* value of <0.05 were considered statistically significant.

RESULTS

Anti-HCV effect of YM-53601. We began to explore the role of the cholesterol biosynthetic pathway in the HCV life cycle by using an SQS inhibitor, YM-53601. We first examined whether HCV

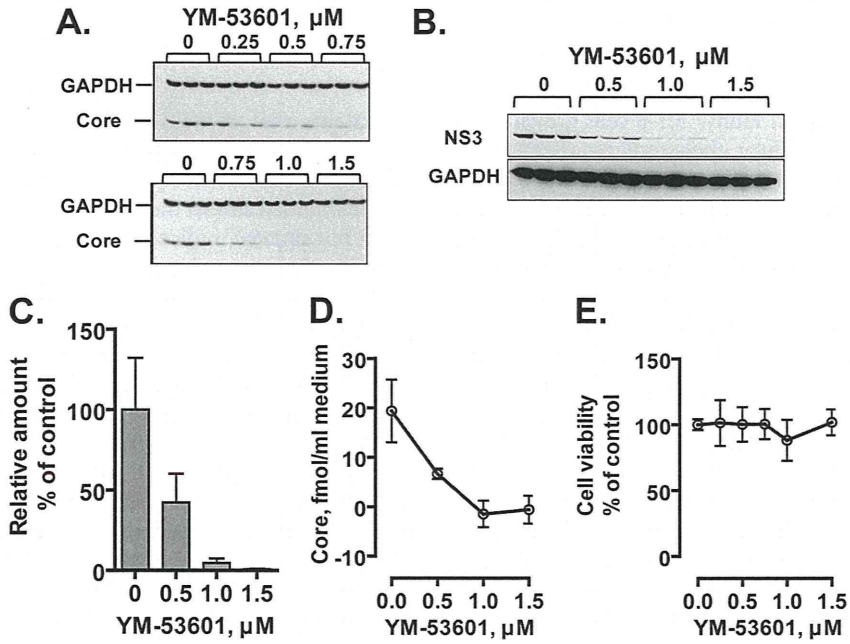

FIG 3 YM-53601 inhibits HCV production without affecting cell viability. Huh-7.5.1-8 cells were infected with HCV JFH-1 and then treated with increasing concentrations of YM-53601 (0 to 1.5 μM) in serum-free medium. The cells and culture supernatants were harvested on the fifth day postinfection. (A and B) An equal portion of each cell lysate was subjected to immunoblotting for core, NS3, and GAPDH proteins. The results from one representative experiment performed in triplicate are shown. Similar results were obtained in four independent experiments. For panel A, samples were run on two blots and are partially redundant. (C) Total RNA fractions were prepared from cells, and then viral and GAPDH RNAs were quantified by RT-qPCR analysis using specific primers for the core and GAPDH sequences, respectively. The amounts of viral RNA relative to that of GAPDH mRNA are expressed as a percentage of the control value and plotted as a function of the drug concentration. (D) The amount of secreted viral particles in each culture supernatant was determined by ELISA for the core protein and plotted as in panel C. (E) Cell viability was determined by XTT assay and expressed and plotted as in panel C. The data in each graph are means ± standard deviations (SD) for triplicate samples from one representative experiment. Similar results were obtained in two or more independent experiments.

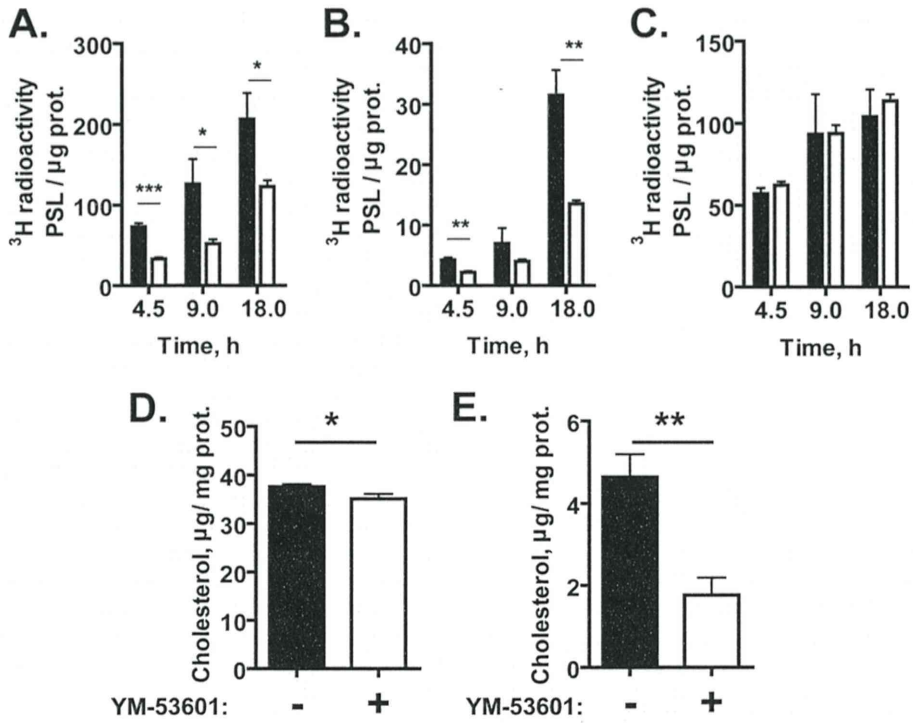

FIG 4 YM-53601 inhibits *de novo* synthesis of cholesterol and cholesteryl esters. (A to C) Huh-7.5.1-8 cells were pretreated with 1 μM YM-53601 (white bars) or its vehicle, DMSO (black bars), in serum-free medium for 24 h. The cells were subsequently labeled using [^{3}H]acetate in the same medium as for the pretreatment for the indicated periods of time. The lipid fractions were extracted from the cells and analyzed by TLC. The incorporation of [^{3}H]acetate into cholesterol (A), cholesteryl esters (B), and triglycerides (C) was quantified and expressed as photostimulated luminescence (PSL) values per μg cellular protein. (D and E) Huh-7.5.1-8 cells were treated with 1 μM YM-53601 (white bars) or DMSO (black bars) for 7 days in serum-free medium. The lipid fraction was extracted from the cells, and the contents of cholesterol (D) and cholesteryl esters (E) were determined. The values for cholesteryl esters (E) are expressed as the cholesterol content in the fraction. Data are means ± SD for triplicate samples from one representative experiment. Similar results were obtained in two independent experiments. *, $P < 0.05$; **, $P < 0.01$; ***, $P < 0.001$.

JFH-1 can replicate efficiently in Huh-7.5.1-8 cells grown under serum-free conditions where cellular cholesterol requirements are met only through *de novo* synthesis. The amounts of viral core and NS3 proteins in JFH-1-infected cells clearly increased from the fourth to sixth day postinfection, compared with that of GAPDH protein (Fig. 2A). Similarly, the amount of secreted viral particles increased during the time course (Fig. 2B). These results indicate that the virus replicates efficiently under the serum-free conditions.

We next examined the effect of YM-53601 on JFH-1 virus production in Huh-7.5.1-8 cells grown under serum-free conditions. The amounts of core (Fig. 3A) and NS3 (Fig. 3B) proteins relative to that of GAPDH protein in infected cells were decreased by the drug treatment in a dose-dependent manner and nearly reached the background level at ≥1 μM. Similarly, the relative amount of intracellular viral RNA (Fig. 3C) and the amount of secreted viral particles (Fig. 3D) were decreased by the drug treatment. The IC_{50} for virus secretion calculated from multiple experiments was 0.16 ± 0.10 μM ($n = 4$). In contrast, cell viability was not affected by the drug at up to 1.5 μM (Fig. 3E). These results indicate that YM-53601 inhibits HCV production in Huh-7.5.1-8 cells without affecting cell viability. The drug also inhibited HCV production from Huh-7.5.1-8 cells grown in serum-containing medium (data not shown) with a slightly higher value of IC_{50} (0.57 ± 0.66 μM; $n = 4$).

To evaluate the effect of YM-53601 on the infectivity of progeny virus, we inoculated naive Huh-7.5.1-8 cells with culture supernatants that contained viral particles secreted from drug-treated (1 μM) and untreated cells. When the inoculum dose was adjusted to contain an equal amount of core protein, these supernatants yielded almost the same amount of progeny viral particles (data not shown), indicating that the drug does not alter the infectivity of progeny virus.

YM-53601 inhibits cholesterol biosynthesis. To test whether YM-53601 inhibits *de novo* synthesis of cholesterol, we pretreated Huh-7.5.1-8 cells with a 1 μM concentration of the drug in serum-free medium for 24 h and then labeled them with [^{3}H]acetate for up to 18 h in the same medium. The drug treatment led to a 40 to 60% reduction in the incorporation of [^{3}H]acetate into cellular cholesterol (Fig. 4A) and its major metabolites, cholesteryl esters (Fig. 4B), compared with the control treatment. In contrast, the incorporation into triglycerides was not affected by the drug (Fig. 4C), indicating a specific effect of YM-53601 on cholesterol biosynthesis. We also determined the cellular contents of cholesterol and cholesteryl esters in Huh-7.5.1-8 cells treated with 1 μM YM-53601 in serum-free medium. The contents of cholesterol (Fig. 4D) and cholesteryl esters (Fig. 4E) in the drug-treated cells were significantly decreased to 93.5% and 38.0%, respectively, of those in the untreated cells. Collectively, these results confirm that YM-53601 inhibits *de novo* cholesterol biosynthesis at the antiviral concentrations.

SQS is an anti-HCV target. To further test whether cellular SQS is important for HCV production, we first investigated the

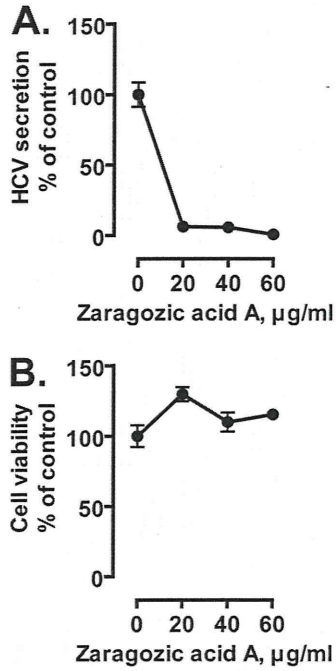

FIG 5 Anti-HCV effect of another SQS inhibitor, zaragozic acid A. Huh-7.5.1-8 cells were infected with HCV JFH-1 and then treated with 0 to 60 μg/ml of zaragozic acid A for 4 days. In this experiment, drug treatment was performed in complete medium because the drug was toxic to cells in serum-free medium. (A) The amount of secreted viral particles in each culture supernatant was determined by ELISA for the core protein. (B) Cell viability was determined by XTT assay. Data in each graph are expressed as a percentage of the control value (without the drug) and are means ± SD for triplicate samples from one representative experiment. Similar results were obtained in two independent experiments. Some error bars are not visible due to their small sizes.

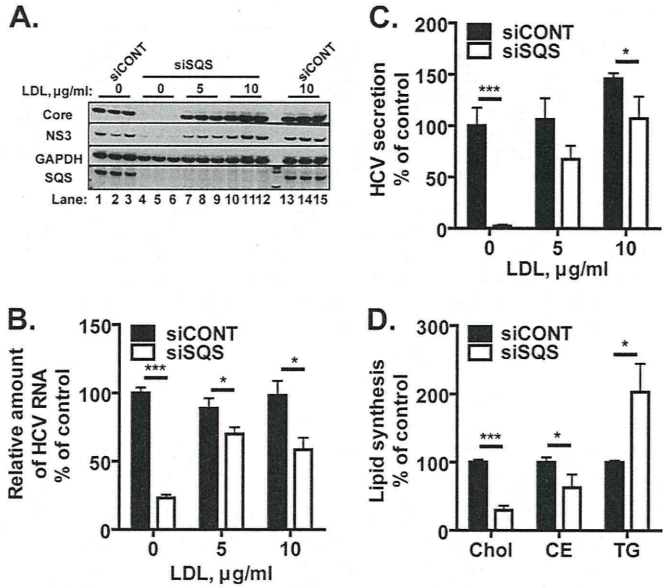

FIG 6 Anti-HCV effect of siRNA-mediated knockdown of SQS and its reversal by the addition of LDL. (A to C) Huh-7.5.1-8 cells were infected with HCV JFH-1 and then incubated in complete medium. On the first day postinfection, the cells were transfected with an siRNA for SQS (siSQS) or a control siRNA (siCONT), and then they were further incubated in serum-free medium that contained 0, 5, and 10 μg/ml of LDL for 4 days. (A) An equal portion of each cell lysate was subjected to immunoblotting for core, NS3, GAPDH, and SQS proteins. The results from one representative experiment performed in triplicate are shown. Similar results were obtained in two independent experiments. (B) Total RNA fractions were isolated from siSQS-transfected (white bars) or siCONT-transfected (black bars) cells, and then HCV RNA was quantified by RT-qPCR analysis using specific primers for the NS5B sequence. The amount of viral RNA relative to that of GAPDH mRNA is expressed as a percentage of the control value (siCONT without LDL) and plotted as a function of the LDL concentration. (C) The amount of secreted viral particles in each culture supernatant was determined by ELISA for the core protein. The concentration of core protein is expressed and plotted as in panel B. (D) Huh-7.5.1-8 cells were transfected with siSQS (white bars) or siCONT (black bars) and subsequently labeled using [^{3}H]acetate in serum-free medium for 18 h. The lipid fractions were extracted from the cells and analyzed by TLC. The incorporation of [^{3}H]acetate into cholesterol (Chol), cholesteryl esters (CE), and triglycerides (TG) was quantified and expressed as a percentage of the control value. Note that the value for cholesteryl esters of siSQS-transfected cells includes in part the incorporation of unidentified metabolites located immediately below the cholesteryl esters on a TLC plate. These metabolites accumulated only in siSQS-transfected cells for unknown reasons. The data in panels B, C, and D are means ± SD for triplicate samples from one representative experiment. Similar results were obtained in at least two independent experiments. *, $P < 0.05$; ***, $P < 0.001$.

effects of another SQS inhibitor, zaragozic acid A (squalestatin S1), on HCV production. The drug decreased the amounts of core and NS3 proteins and viral RNA (data not shown) and progeny virus production (Fig. 5A) without affecting cell viability (Fig. 5B), indicating that zaragozic acid A inhibits HCV production as well as YM-53601.

We next investigated the effect of siRNA-mediated knockdown of SQS on HCV production. Huh-7.5.1-8 cells were infected with HCV JFH-1 and then transfected with either an siRNA against SQS (siSQS) or a control siRNA (siCONT). Transfection with siSQS resulted in almost complete depletion of cellular SQS compared with transfection with siCONT (Fig. 6A, bottom row). The amounts of core and NS3 proteins relative to GAPDH protein in the siSQS-transfected cells were markedly lower than those in the control cells (Fig. 6A, compare lanes 4 to 6 with lanes 1 to 3). The relative amounts of intracellular viral RNA (Fig. 6B, left pair of bars) and secreted viral particles (Fig. 6C, left pair of bars) were also decreased in the siSQS-transfected cells. A similar antiviral effect was observed with another siRNA for SQS (a Stealth RNAi siRNA, HSS103616) (data not shown). These results indicate that siRNA-mediated knockdown of SQS leads to reduced HCV production.

A metabolic labeling experiment with [^{3}H]acetate confirmed that transfection with siSQS causes a specific decrease in cholesterol biosynthesis (Fig. 6D). To rescue the defective cholesterol biosynthesis, we added LDL (final concentrations, 5 and 10 μg/ml) to the medium of HCV-infected cells after siSQS transfection. The inhibition of virus production by siSQS was reversed by the addition of LDL (Fig. 6A to C), suggesting that the antiviral effect is attributable to a decrease in cellular contents of cholesterol and/or cholesteryl esters. Consistent with this, the inhibition of virus production by YM-53601 was also reversed significantly by the addition of LDL as judged by intracellular viral protein levels (Fig. 7).

Collectively, these results demonstrate that SQS is a potential target for anti-HCV strategies.

An ACAT inhibitor does not show an anti-HCV effect. The degree of decrease in the cholesteryl ester content after treatment with YM-53601 (Fig. 4E) was substantially higher than that in the cholesterol content (Fig. 4D), raising the possibility that biosyn-

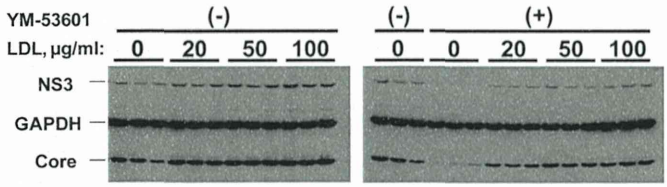

FIG 7 The anti-HCV effect of YM-53601 is significantly reversed by LDL. Huh-7.5.1-8 cells were infected with HCV JFH-1 and then treated with 1 μM YM-53601 or DMSO in serum-free medium that contained 0 to 100 μg/ml of LDL for 5 days. An equal portion of each cell lysate was subjected to immunoblotting for core, NS3, and GAPDH proteins. The results from one representative experiment performed in triplicates are shown. Similar results were obtained in two independent experiments.

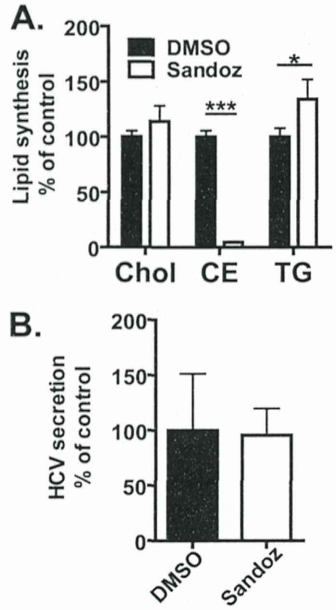

FIG 8 An ACAT inhibitor, Sandoz 58-035, does not exhibit an anti-HCV effect. (A) Huh-7.5.1-8 cells were pretreated with 30 μM Sandoz 58-035 or its vehicle, DMSO, in serum-free medium for 24 h. The cells were subsequently labeled using [^{3}H]acetate in the same medium as for the pretreatment for 18 h. The lipid fractions were extracted from cells and separated by TLC. The incorporation of [^{3}H]acetate into cholesterol (Chol), cholesteryl esters (CE), and triglycerides (TG) was quantified and expressed as a percentage of the control value. (B) Huh-7.5.1-8 cells were infected with HCV JFH-1 and then treated with Sandoz 58-035 or DMSO (control) under the same conditions as described above. The culture supernatants were harvested on the fifth day postinfection. The amount of secreted viral particles in each culture supernatant was determined by ELISA for the core protein and is expressed as a percentage of the control value. Data in each graph are means ± SD for triplicate samples from one representative experiment. Similar results were obtained in two independent experiments. *, $P < 0.05$; ***, $P < 0.001$.

thesis of cholesteryl esters is more important for HCV production than that of cholesterol. To test this possibility, we examined the effect of Sandoz 58-035, an inhibitor of acyl-CoA:cholesterol acyltransferase (ACAT) that catalyzes the biosynthesis of cholesteryl esters from cholesterol and fatty acyl-CoA, on HCV production. A metabolic labeling experiment with [^{3}H]acetate verified that treatment with 30 μM Sandoz 58-035 inhibits cholesteryl ester synthesis but not cholesterol and triglyceride syntheses in Huh-7.5.1-8 cells grown in serum-free medium (Fig. 8A). When Huh-7.5.1-8 cells were infected with HCV JFH-1 and then treated with either 30 μM Sandoz 58-035 or DMSO (control) in serum-free medium, virus secretion from the drug-treated cells was similar to that from the control cells (Fig. 8B). Taken together with the results shown in Fig. 3 and 4, these results suggest that biosynthesis of cholesterol, but not that of cholesteryl esters, is important for HCV production.

YM-53601 inhibits RNA replication of HCV JFH-1. To investigate which stages of the HCV life cycle are targeted by YM-53601, we conducted a transient-replication assay using a subgenomic replicon, SGR-JFH1/Luc (45). When cells are transfected with this replicon RNA, the self-encoded viral RNA replicase (NS3-NS5B) is expressed under the control of the EMCV IRES and then amplifies the replicon in the cells. The replicon also encodes luciferase translated under HCV IRES control, thereby allowing quantitation of viral RNA replication and translation activities via luciferase expression. Parallel transfection with a replication-incompetent mutant replicon, SGR-JFH1/Luc-GND (45), enables estimation of the level of replication-independent luciferase expression from the input replicon. As shown in Fig. 9A, luciferase activity in the wild-type replicon-transfected cells reached its peak at 47 h posttransfection and then declined. In the presence of YM-53601, the peak activity was decreased to approximately half of that in the control cells. The mutant replicon yielded very low luciferase activity irrespective of the drug treatment, confirming that the activity yielded by the wild-type replicon at 23 to 71 h posttransfection was dependent on viral RNA replication. Multiple experiments showed that the drug treatment lowered the luciferase activity at 46 to 50 h posttransfection to 52.6% ± 11.3% (mean ± standard error of the mean [SEM]; $n = 5$) of the control activity.

To test whether YM-53601 inhibits HCV IRES-dependent translation, we transfected drug-pretreated Huh-7.5.1-8 cells with the replication-incompetent mutant replicon SGR-JFH1/Luc-GND and then monitored luciferase expression in the presence of the drug for up to 21 h. Because the replicon cannot be replicated, luciferase activity yielded by the mutant replicon is attributable exclusively to HCV IRES-dependent translation and reflects the residual amount of the input replicon RNA. As shown in Fig. 9B, luciferase activity in the drug-treated cells and untreated control cells reached its peak at 3 h posttransfection and then declined. During the time course, the activity in the drug-treated cells was not lower, but rather was higher, than the activity in the control cells. Furthermore, the level of NS3 protein that was expressed from the mutant replicon changed similarly in the drug-treated and control cells, reaching its peak at 3 to 6 h posttransfection (Fig. 9C). Thus, it appears unlikely that YM-53601 impairs HCV IRES-dependent translation or viral RNA and NS protein stability.

Taken together, these results suggest that YM-53601 inhibits the RNA replication of HCV JFH-1.

YM-53601 does not affect the cellular distribution of NS4B protein. It is possible that YM-53601 alters the formation of the HCV-specific ultrastructure termed the membranous web, which serves as a scaffold for the viral RNA replication complex (55, 56), thereby inhibiting viral RNA replication. To test this possibility, we treated Huh-7.5.1-8 cells stably expressing HA-tagged NS4B protein with YM-53601 for 3 days in serum-free medium. It has been shown that the membranous web is induced by NS4B protein alone (55, 57) and appears as NS4B-accumulating foci or dots under fluorescence microscopy (58, 59). We found small intense foci that were detected with an anti-HA antibody in non-drug-treated cells (Fig. 10C) and are similar to the NS4B foci previously